The Fatigue Design of a Bone Preserving Hip Implant With Functionally Graded Cellular Material

Sajad Arabnejad Khanoki

Damiano Pasini

Department of Mechanical Engineering,
McGill University

1 Background

An orthopaedic hip implant is expected to support dynamic forces generated by human activities. To avoid progressive and localized damage caused by daily cyclic loading, the prosthesis is to be designed for fatigue under high cycle regime. Recently, a methodology has been developed to design a novel hip implant made of a cellular material with a periodic microarchitecture [1]. In contrast to current hip replacement implants typically made out of a fully solid material, which can be coated with a porous layer, this implant is completely porous. The microarchitecture of the material is a lattice displaying graded property distribution. The advantage of controlling the microarchitecture is twofold. First, the overall implant can be designed to be more compliant, which reduces stress shielding and bone resorption [2]. Second, the material porosity can be optimized to reduce bone-implant interface stresses, thereby lowering implant micromo-tion. Although encouraging, these results have been obtained by applying a static loading regime to the implant, thus neglecting the impact of an applied cyclic loading. In this paper, the methodology [1] is extended to design the femoral implant against fatigue fracture caused by the cyclic loading as a result of walking.

2 Methods

Figure 1 summarizes the procedure proposed here to design a graded cellular implant against fatigue fracture. The approach combines multiscale mechanics and multiobjective optimization. The former deals with the scale-dependent material structure; the latter handles the conflicting nature of bone resorption and implant interface stress. As fatigue failure theory, we use here the Soderberg's criterion in the procedure to design the implant for infinite fatigue life. The main steps illustrated in Fig. 1 are here briefly described:

- (1) A finite element model of the bone is created by processing CT-scan data of a patient bone.
- (2) A lattice unit cell is considered as the building block of the implant. The unit cell properties are obtained through asymptotic homogenization (AH). The homogenized elastic tensor E^H_{ijkl}, and yield surfaces $\bar{\sigma}^y_{ij}$ of the cell topology under multi-axial loading conditions are calculated. A detailed description of the homogenization procedure and the steps required to calculate the effective mechanical properties are given in [1].
- (3,4) From FEA, the mean and alternative macroscopic stresses are obtained and used in the Soderberg's fatigue criterion to determine the design safety factor (SF).
- (5) Two conflicting objective functions, bone resorption $m_r(\boldsymbol{b})$ and interface failure index $F(\boldsymbol{b})$, are minimized via a multiobjective optimization strategy subjected to a set of inequality constraints. The amount of bone resorption is determined by comparing the local strain energy per unit of bone mass between the preoperative and the postoperative situation, as described in detail in [1]. On the other hand, the interface failure index $F(\boldsymbol{b})$ is expressed as:

$$F(\boldsymbol{b}) = \max\left\{\frac{f(\sigma)_i}{\frac{1}{A}\int_A f(\sigma)_i dA}\right\} \tag{1}$$

where i is the loading case (1, 2, and 3), and A is the interface area. $f(\sigma)$ is defined as the interface failure caused by shear stress. It is expressed as τ/S_s, where $\boldsymbol{\tau}$ is the local shear stress at the bone-implant interface, and S_s is the bone shear strength which can be obtained by the power law relation used by Pal et al. [3] ($S_s = 21.6\,\rho^{1.65}$).
- (6) The design variables are the relative density at the sampling points of the implant domain shown in red in Fig. 1. They are collected in the vector $\boldsymbol{b}$ of design variables. The components of $\boldsymbol{b}$ are updated until the set of non-dominated solutions of the Pareto front is obtained. The optimization algorithm used here is the non-dominated sorting genetic(NSGA-II) [4].

The distal end of the femur is fixed to avoid rigid-body motion. Three loading cases, 1, 2, and 3, representing the cyclic load during walking are applied to the hip joint and the abductor [5, 6]. Magnitude and direction of the hip joint and the abductor forces (given in brackets in the following text), are with respect to the load cases: 1) 2317 N at 24 deg from vertical (702 N at 28 deg from vertical), 2) 1158 N at 15 deg from vertical (351 N at 8 deg from vertical), 3) 1548 N at 56 deg from vertical (468 N at 35 deg from vertical).

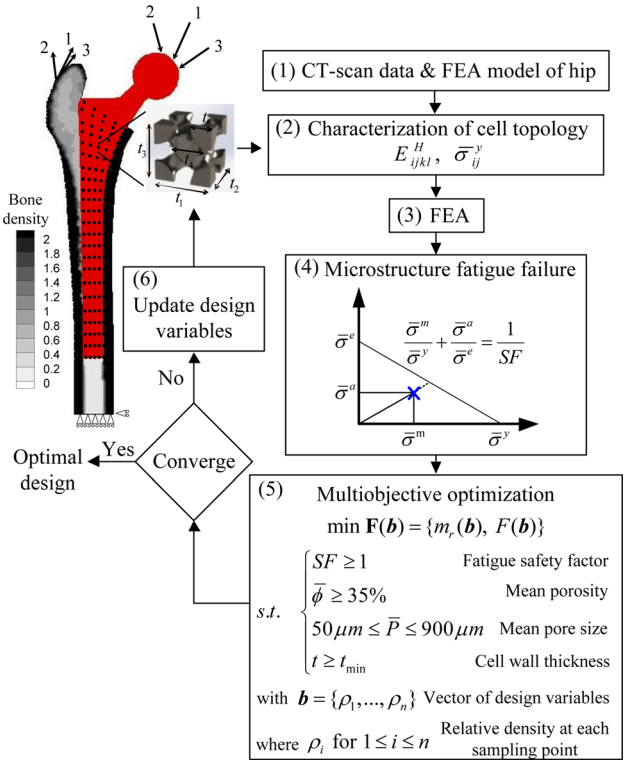

Fig. 1 Flow chart illustrating the design methodology to obtain an optimum graded cellular material for hip replacement implants

Manuscript received March 15, 2013; final manuscript received April 24, 2013; published online June 5, 2013. Editor: Arthur G. Erdman.

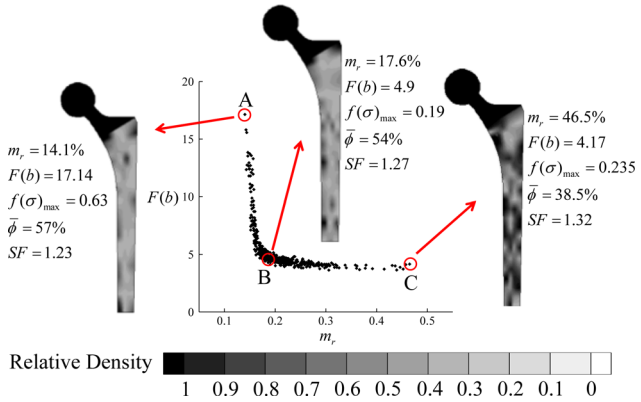

Fig. 2 Trade-off distributions of relative density for a planar hip implant

3 Results

The methodology described above is applied for the design of a 2D graded cellular implant. For the purpose of a preliminary study, the 3D geometry of the femur is simplified to a 2D model, which is assumed to have a side plate of variable thickness [6]. This choice helps reduce the computational cost involved in the optimization process. Nevertheless, many of the essential features of the implant physics can be still captured with a 2D model. For mid-frontal loadings, von Mises and interface stresses distribution can be captured with a reasonable accuracy, similar to the results predicted by a full 3D model [6]. In this exploratory study, a square cell topology has been considered as the building block of the implant material. In a future work, alternative cell topologies suitable for bone tissue scaffolding will be used in the coating layer of the implant.

CT scan data of a 38-year-old male, obtained through the visible human project (VHP), is used to construct the 2D model of the femur. The apparent density (ρ) of each bone element is determined by a linear relation between the Hounsfield value (HU) and the density [7]. ANSYS (Canonsburg, Pennsylvania, U.S.A) is used to build, mesh, and solve the 2D model via a linear analysis. Figure 2 shows the Pareto frontier obtained after 25000 function evaluations. All the optimum relative density distributions for the hip stem implant designed with square cell topology are also shown. The x axis represents the amount of bone resorption for the implanted hip; the interface failure index is on the y axis.

4 Interpretation

In this section, we compare the performance of a fully dense titanium implant and the graded cellular implant in terms of bone resorption and interface shear stress. We select solutions B (Fig. 2) for the comparison. As shown in Fig. 3, the initial postoperative configuration of bone loss for the fully solid is about 53.8% higher than that of the lattice implant. The maximum shear interface failure at the distal end of solution B has also reduced significantly, of about 79%. This shows that the design of a more flexible implant through the concept of a graded cellular material has the beneficial effect of improving the load-sharing capacity of the implant, thereby reducing bone resorption. The optimized graded distribution of stiffness properties can also reduce the peak of stress-interface stress.

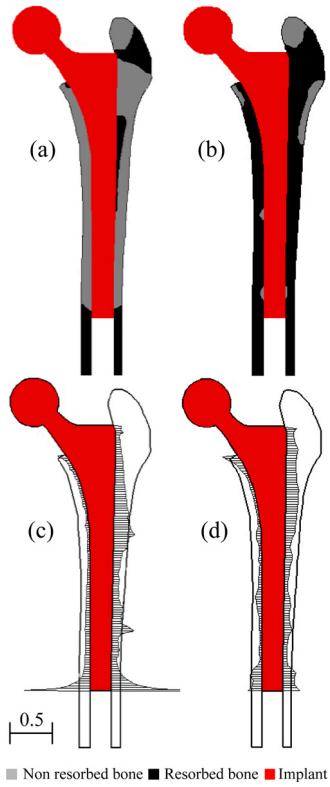

Fig. 3 Distribution of bone resorption and shear interface failure *f*(σ) around (*a*, *c*) fully dense titanium implant, (*b*, *d*) graded cellular implant (solution B in Fig. 3)

The work of this paper presented a method to design a hip implant with variable stiffness properties. Compared to a fully-dense titanium implant, the optimized cellular implant exhibits a reduction of 53.8% of bone resorption and 79% of interface failure, showing that this concept can significantly contribute to reduce some clinical consequences of current implants.

References

[1] Khanoki, S. A., and Pasini, D., 2012, "Multiscale Design and Multiobjective Optimization of Orthopedic Hip Implants With Functionally Graded Cellular Material," J. Biomech. Eng., **134**(3), p. 031004.

[2] Glassman, A., Bobyn, J., and Tanzer, M., 2006, "New Femoral Designs Do They Influence Stress Shielding?," Clin. Orthop. Relat. Res., **453**(12), pp. 64–74.

[3] Pal, B., Gupta, S., and New, A., 2009, "A Numerical Study of Failure Mechanisms in the Cemented Resurfaced Femur: Effects of Interface Characteristics and Bone Remodelling," Proc. Inst. Mech. Eng., Part H: J. Eng. Med., **223**(4), pp. 471–484.

[4] Deb, K., Pratap, A., Agarwal, S., and Meyarivan, T., 2002, "A Fast and Elitist Multiobjective Genetic Algorithm: NSGA-II," IEEE Trans. Evol. Comput., **6**(2), pp. 182–197.

[5] Carter, D., Orr, T., and Fyhrie, D., 1989, "Relationships Between Loading History and Femoral Cancellous Bone Architecture," J. Biomech., **22**(3), pp. 231–244.

[6] Weinans, H., Huiskes, R., and Grootenboer, H., 1994, "Effects of Fit and Bonding Characteristics of Femoral Stems on Adaptive Bone Remodeling," ASME J. Biomech. Eng., **116**(4), pp. 393–400.

[7] Taylor, W. R., Roland, E., Ploeg, H., Hertig, D., Klabunde, R., Warner, M. D., Hobatho, M. C., Rakotomanana, L., and Clift, S. E., 2002, "Determination of Orthotropic Bone Elastic Constants Using FEA and Modal Analysis," J. Biomech., **35**(6), pp. 767–773.